

LETTERS

Pyramidal Structures of Lanthanide–C₆₀ Clusters (Ln_n(C₆₀)_m: Ln = Eu and Ho)

Satoshi Nagao, Yuichi Negishi, Akiko Kato, Yoshiaki Nakamura, and Atsushi Nakajima*

Department of Chemistry, Faculty of Science and Technology, Keio University, 3-14-1 Hiyoshi, Kohoku-ku, Yokohama 223-8522, Japan

Koji Kaya

Department of Chemistry, Faculty of Science and Technology, Keio University, 3-14-1 Hiyoshi, Kohoku-ku, Yokohama 223-8522, Japan, and Institute for Molecular Science, Myodaiji, Okazaki, 444-8585, Japan

Received: July 28, 1999; In Final Form: September 14, 1999

Novel lanthanide organometallic clusters, Ln_n(C₆₀)_m, consisting of lanthanide atoms (Ln; Ln = Eu and Ho) and C₆₀ molecules were produced in gas phase by a two-laser vaporization method. The Ln_n(C₆₀)_m clusters were produced predominantly at compositions of (n, m) = (n, n + 3) [n = 1–4]. These stoichiometries showed no chemisorption reactivity toward CCl₄ and O₂ reactants. The cluster having (1, 4) composition is proposed to form a tetrahedral structure, in which a Ln atom is surrounded by four C₆₀ molecules. In larger clusters with (n, n + 3) composition, each Ln atom is found in a local (1, 4) group. Together with the results of sequential chemisorption of Cl atoms on cluster cations, photoelectron spectroscopy of cluster anions leads us to conclude that Ln₁(C₆₀)_m clusters are charge-transfer complexes expressed as Ln₁^{x+}(C₆₀)_m^{x-}, and that Eu and Ho atoms exist as Eu²⁺ and Ho³⁺ ions, respectively.

1. Introduction

The successful synthesis of the C₆₀ molecule has opened a way to create modified fullerenes.¹ An important discovery in this respect was that of superconductivity at rather high temperatures in the alkaline–C₆₀ solids.^{2,3} There has been intensive research activity in the field of chemically modified fullerenes, specifically fullerenes containing encapsulated atoms.^{4–17} C₆₀-based charge-transfer clusters are one of the promising candidates for the synthesis of novel compounds with tailored properties, which include superconducting and optical properties. Since it has been expected that donor elements of the groups 1, 2, and 13 as well as lanthanides and actinides can form stable charge-transfer complexes with the fullerenes, there

have been a number of experiments on the formation and the characterization of their metallofullerides.

For lanthanide fullerides, a report of the superconducting Yb_{2.5}C₆₀ phase provides incentive for synthesizing other lanthanide C₆₀ fullerides.¹⁸ The lanthanide donor atoms are ionized, resulting in the release of electrons to form negatively charged fullerenes. In the ytterbium fulleride, moreover, there is evidence for short-range, covalent interactions, which suggests that lanthanides do not react with the fullerenes according to a simple intercalation reaction, but react to form covalently bound lanthanide fullerides where the lanthanide ion interacts strongly with the fullerene. To obtain materials with better-defined structures, it is worthwhile to investigate the interaction of fullerenes with lanthanides in a controlled way. Making lanthanide fullerides in the gas phase may allow us to prepare well-defined deposited materials. There is much more fullerene

* Corresponding author.

chemistry to be explored, and the investigation of rare-earth fullerides may open up a new field of organolanthanide chemistry.

The application of laser vaporization to the gas-phase synthesis of organometallic compounds enables us to prepare the constituents without the interfering effects of solvents, aggregation phenomena, and counterions. In this letter, we present results on the gas-phase synthesis of lanthanide fullerides for Eu and Ho. Mass spectrometry, photoelectron spectroscopy, and chemical probe techniques have been applied to reveal information on their geometric and electronic structures, especially the oxidation states of the lanthanide atom. We find donor elements of lanthanides to form stable charge-transfer clusters along with superstructures composed of multi-lanthanide atoms and multi-C₆₀ molecules, where Eu and Ho can work as divalent and trivalent atoms, respectively.

2. Experimental Section

Details of the experimental setup were previously described elsewhere.^{19,20} Briefly, lanthanide (Ln; Ln = Eu or Ho)-C₆₀ binary clusters were produced in the gas phase by laser vaporization using the second harmonic of two pulsed Nd³⁺:YAG lasers (wavelength = 532 nm). Each laser was focused onto a rotating and translating rod; one was a lanthanide metal rod, and the other was a C₆₀ rod. The energy of the vaporization laser was 10–15 mJ/pulse for the Ln metal rod and 70–100 μJ/pulse for the C₆₀ rod. The laser vaporization of C₆₀ was very sensitive to the laser energy. For example, a laser energy of more than 200 μJ/pulse resulted in noticeable fragmentation of C₆₀ via “C₂ loss”. Consequently, the laser vaporization of the C₆₀ rod should occur downstream from that of the metal rod because the reverse order results in the fragmentation of C₆₀ due to the high laser fluence for the metal rod. The hot vapors of Ln and C₆₀ were quenched to room temperature by a pulsed He carrier gas (5–6 atm stagnation pressure), and Ln-C₆₀ clusters were generated. After the cluster beam was skimmed, the neutral clusters were ionized in a static electric field by an ArF excimer laser (6.42 eV), whereas the positive or negative ions were accelerated with a pulsed electric potential to 4 kV without photoionization. The ions were mass-analyzed by a time-of-flight (TOF) mass spectrometer with a reflectron. To detect heavy cluster ions efficiently, an ion detector known as an “Even-cup” was used.²¹

Chemical probe measurements were made using a conventional flow-tube reactor.²² Inside the flow-tube reactor, O₂ or CCl₄ seeded in He was injected in synchronization with the flow of the clusters, and the adducts of Ln-C₆₀ clusters were also mass-analyzed.

The PES spectra of the target anions were measured using an apparatus equipped with a magnetic bottle TOF photoelectron spectrometer.²³ The Ln-C₆₀ clusters were similarly generated by the two-laser vaporization, and only the cluster anions were accelerated to 900 eV. After being selected by a mass gate, the target anions were decelerated and photodetached with the fourth harmonic (266 nm; 4.66 eV) of a Nd³⁺:YAG laser. The photoelectron signal was typically accumulated to 15000–30000 shots. The obtained energy resolution was about 20 meV fwhm at 1 eV electron energy. The energy of the photoelectron was calibrated by measuring photoelectron spectra of Au⁻.^{24,25} The laser power for photodetachment was in the range of 3–5 mJ/cm², and no power-dependent processes for the spectrum shape were observed.

3. Results and Discussion

Figure 1 shows mass spectra of (a) Eu_n(C₆₀)_m⁺ and (b)

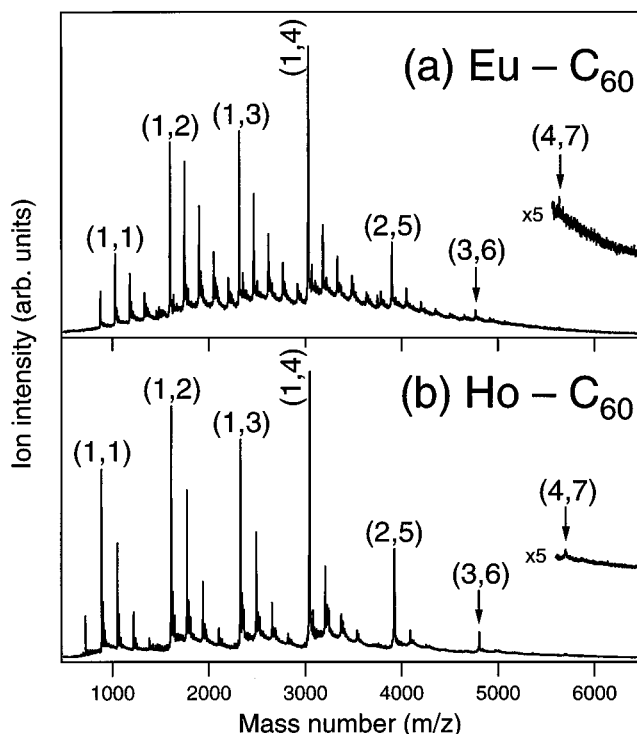


Figure 1. Time-of-flight mass spectra of (a) Eu-C₆₀ and (b) Ho-C₆₀ cluster cations. Peaks of the cluster cations are labeled according to the notation (n, m) , denoting the number of metal atoms (n) and C₆₀ molecules (m).

Ho_n(C₆₀)_m⁺ cluster cations produced by the ablation of Ln (Ln = Eu or Ho) and C₆₀ targets. Peaks of the cationic clusters are labeled according to the notation, $(n, m)^+$, denoting the number of Ln atoms (n) and C₆₀ (m). Under the prevalent conditions, the contribution of Ln_n⁺ cluster to Ln_n(C₆₀)_m⁺ formation was negligible because the abundance of the Ln_n⁺ clusters ($n \geq 2$) was less than 1/1000 that of the Ln⁺ atoms. Both mass spectra indicate a common pattern of prominent peaks (i.e., “magic number”). The prominent peaks in the mass spectra correspond to $(n, m) = (1, 1)^+, (1, 2)^+, (1, 3)^+, \text{ and } (1, 4)^+, (2, 5)^+, (3, 6)^+, \text{ and } (4, 7)^+$, which are expressed as $(1, m)^+ [m = 1-3]$ and $(n, n + 3)^+ [n = 1-4]$ have common structures. The mass distribution of the prominent clusters remained unchanged even when the concentration of Ln atoms was increased with higher laser fluence for the Ln rod. Moreover, we observed similar patterns in the mass spectra of anionic and neutral as well as the cationic Ho-C₆₀ clusters. This implies that all of the cationic, anionic, and neutral Ln-C₆₀ clusters composed of $(1, m) [m = 1-3]$ and $(n, n + 3) [n = 1-4]$ have common structures. The magic numbers for Ln-C₆₀ cluster cations are different from those of the other organometallic clusters such as M₇-C₆₀,²⁰ M₇-C₆H₆,²⁶ and Ln-C₈H₈.²⁷ Since the bonding in Ln-C₆₀ clusters was expected to be ionic, we performed a chemical probe experiment using CCl₄ as reactant to deduce their geometric structures and charge distributions.

Figure 2 shows the mass spectra of Ho-C₆₀ cluster cations (a) after and (b) before the reaction toward CCl₄ seeded in He gas. The clusters composed of $(n, n + 3)^+$ and C₆₀⁺ itself were nonreactive toward CCl₄, while the others were reactive, resulting in the formation of Cl-atom adducts (Ho_n(C₆₀)_mCl_k⁺). Here, it is assumed that the Cl⁻ ion, generated through the dissociation of CCl₄, is concerned in the formation process. Dissociative electron attachment from the cluster might be most conceivable, where CCl₄ dissociates into Cl⁻ and CCl₃. It is reasonably presumed that an exterior Ho atom in Ho_n(C₆₀)_m⁺

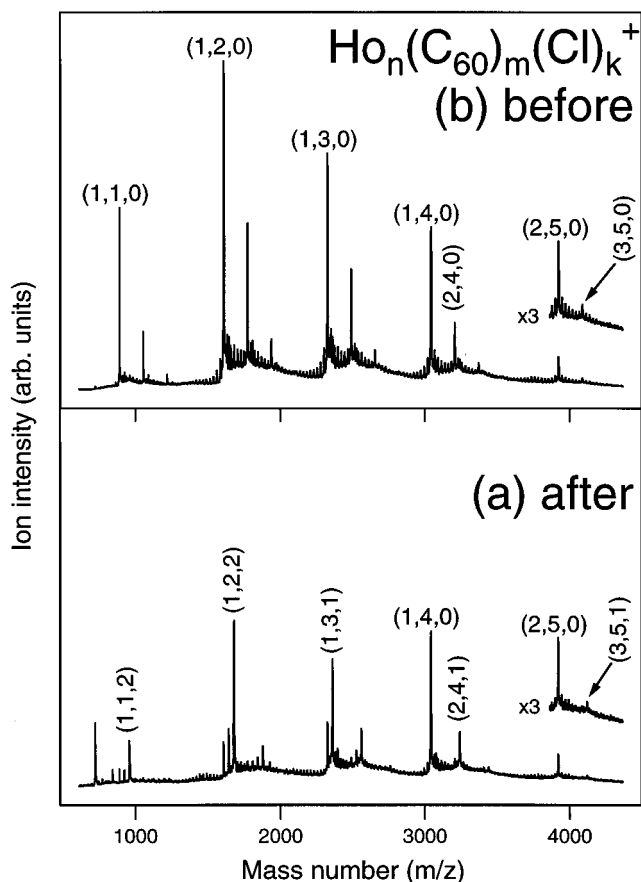


Figure 2. Time-of-flight mass spectra of $\text{Ho}_n\text{-(C}_{60}\text{)}_m\text{-(Cl)}_k^+$ cluster cations (a) after and (b) before the reaction with CCl_4 reactant ($m = 1-5$). Peaks of the cluster cations are labeled according to the notation (n, m, k), denoting the numbers of Ho atoms (n), C_{60} molecules (m), and Cl atoms (k).

is the reaction site for the chloridization because C_{60}^+ itself does not show the chloridization reaction. Similarly, $\text{Ho}_n\text{-(C}_{60}\text{)}_{n+3}^+$ were also nonreactive toward an oxygen molecule (O_2). This lack of reactivity implies that $\text{Ho}_n\text{-(C}_{60}\text{)}_{n+3}^+$ should have no exterior Ho atoms. It is proposed that $\text{Ho}_1\text{-(C}_{60}\text{)}_4^+$ forms a tetrahedral methane-like structure, as shown in Figure 3c, where the Ho atom is geometrically blocked by the surrounding C_{60} s. Since it is reasonably presumed that $\text{Ho}_1\text{-(C}_{60}\text{)}_4^+$ is the smallest unit of $\text{Ho}_n\text{-(C}_{60}\text{)}_{n+3}^+$ species, plausible structures of the other ($n, n+3$) $^+$ follow as in Figure 3d-f. The addition of $\text{Ho}_1\text{-(C}_{60}\text{)}_1$ to $\text{Ho}_1\text{-(C}_{60}\text{)}_4^+$ gives $\text{Ho}_2\text{-(C}_{60}\text{)}_5^+$ (Figure 3d) consisting of two local $\text{Ho}_1\text{-(C}_{60}\text{)}_4$ groups, resulting in a tetracapped trigonal bipyramid. The successive addition of $\text{Ho}_1\text{-(C}_{60}\text{)}_1$ sequentially forms a local $\text{Ho}_1\text{-(C}_{60}\text{)}_4$ group. The composition of $\text{Ho}_n\text{-(C}_{60}\text{)}_{n+3}^+$ can be expressed as $\text{Ho}_{1+j}\text{-(C}_{60}\text{)}_{4+j}^+$ [$j = 0-3$], in which each Ho atom is favorably surrounded by four C_{60} s.

As described above, the anionic and neutral Ho-C_{60} clusters were also produced predominantly at the composition of ($n, n+3$) 0 . They show the same behavior in mass distributions irrespective of different charging states, which indicates that all of the cationic, anionic, and neutral clusters of Ho-C_{60} form the common geometric structures constituting of $\text{Ho}_1\text{-(C}_{60}\text{)}_4$ units. As well as $\text{Ho}_n\text{-(C}_{60}\text{)}_m^+$, $\text{Eu}_n\text{-(C}_{60}\text{)}_m^+$ clusters show almost the same behavior; $\text{Eu}_n\text{-(C}_{60}\text{)}_{n+3}^+$ ($n = 1-4$) are produced abundantly and they are nonreactive toward CCl_4 , suggesting that $\text{Eu}_n\text{-(C}_{60}\text{)}_{n+3}^+$ also consists of the tetrahedral unit of $\text{Eu}_1\text{-(C}_{60}\text{)}_4$. Correspondingly, stability of ($n, n+3$) $^+$ species is generally observed in the lanthanide- C_{60} clusters such as Ce-C_{60} , Nd-C_{60} , Yb-C_{60} , which indicates that the structural unit of (1, 4)

is common among Ln-C_{60} clusters. While (1, 4) takes the tetrahedral structure, (1, 2) and (1, 3) should be regarded as precursors of (1, 4) and they should act as a reaction site toward a gas reactant, as shown in Figure 3, parts a and b. The chemical probe experiment can reveal their structure as described below.

In general, the lanthanide complexes are well-known as charge-transfer complexes where the Ln atoms are multiply-charged cations and the ligands are charged anions.²⁷ By analogy of the reported lanthanide complexes, it is conceivable that all of the Ln atoms take the oxidation state of +3 except that Eu and Yb atoms can also take that of +2. Since the C_{60} molecule has a lowest unoccupied molecular orbital (LUMO) which is triply degenerated, it is intriguing to estimate the amount of electrons transferred from the Ln atom to C_{60} molecules in Ln-C_{60} clusters. To deduce the electronic structure of Ln-C_{60} clusters, photoelectron spectroscopy of $\text{Ln}_1\text{-(C}_{60}\text{)}_m^-$ anions were performed. Figure 4 shows the photoelectron spectra of (a) $\text{Eu}_1\text{-(C}_{60}\text{)}_m^-$ and (b) $\text{Ho}_1\text{-(C}_{60}\text{)}_m^-$ at 266 nm (4.66 eV). In the spectra, the horizontal axis corresponds to the electron binding energy, E_b , defined as $E_b = h\nu - E_k$ where E_k is the kinetic energy of the photoelectron. Arrows indicate threshold energies (E_T), which correspond to the upper limit of the adiabatic electron affinity (AEA). The obtained AEAs of $\text{Eu}_1\text{-(C}_{60}\text{)}_m^-$ and $\text{Ho}_1\text{-(C}_{60}\text{)}_m^-$ species are tabulated in Table 1. For $\text{Eu}_1\text{-(C}_{60}\text{)}_3^-$ and $\text{Ho}_1\text{-(C}_{60}\text{)}_4^-$, no effective photodetachment occurs at 266 nm and only lower limits of their AEAs are obtained as 4.0 eV.

When the spectra of $\text{Ln}_1\text{-(C}_{60}\text{)}_m^-$ were compared as a function of the number of C_{60} molecules (m), it was found that the AEA of $\text{Ho}_1\text{-(C}_{60}\text{)}_3^-$ is almost the same to that of $\text{Ho}_1\text{-(C}_{60}\text{)}_2^-$, whereas the AEA of $\text{Eu}_1\text{-(C}_{60}\text{)}_3^-$ is higher than that of $\text{Eu}_1\text{-(C}_{60}\text{)}_2^-$. This difference between Eu-C_{60} and Ho-C_{60} can be explained by the preferred oxidation states of the Ln atoms. Assuming that Eu and Ho atoms become Eu^{2+} and Ho^{3+} , respectively, the allotment of valence electrons in $\text{Ln}_1\text{-(C}_{60}\text{)}_m^-$ anions are expected to be in accordance with the drawing in Figure 5. Here, it is reasonably assumed that the extra electron in the $\text{Ln}_1\text{-(C}_{60}\text{)}_m^-$ anions should be localized on C_{60} . In fact, the theoretical calculation by Nagase et al. indicates that the Ln atom is positively charged in endohedral metallofullerenes such as La@C_{82} and Ce@C_{82} , transferring valence electrons to the fullerene cage.¹³

According to the bonding scheme shown in Figure 5, for Ho-C_{60} the energy difference between the anion and the corresponding neutral, $\text{EA}(\text{Ln}_1\text{-(C}_{60}\text{)}_m^-)$, can simply be estimated by the following equations:

$$\text{EA}(\text{Ho}^{3+}\text{-(C}_{60}\text{)}_2^{3-}) = \text{EA}(\text{C}_{60} \rightarrow \text{C}_{60}^{4-}) - \text{EA}(\text{C}_{60} \rightarrow \text{C}_{60}^{3-}) + \Delta \quad (1)$$

$$\text{EA}(\text{Ho}^{3+}\text{-(C}_{60}\text{)}_2^{3-}) = \text{EA}(\text{C}_{60} \rightarrow \text{C}_{60}^{2-}) - \text{EA}(\text{C}_{60} \rightarrow \text{C}_{60}^-) + \Delta \quad (2)$$

$$\text{EA}(\text{Ho}^{3+}\text{-(C}_{60}\text{)}_3^{3-}) = \text{EA}(\text{C}_{60} \rightarrow \text{C}_{60}^{2-}) - \text{EA}(\text{C}_{60} \rightarrow \text{C}_{60}^-) + \Delta \quad (3)$$

$$\text{EA}(\text{Ho}^{3+}\text{-(C}_{60}\text{)}_4^{3-}) = \text{EA}(\text{C}_{60} \rightarrow \text{C}_{60}^-) + \Delta \quad (4)$$

where Δ is Coulomb binding energy between Ho^{3+} and the charged C_{60} . Apparent from the equations, the EA of (1, 2) and (1, 3) for trivalent Ho is the same, which is consistent with the experimental finding. Furthermore, the increase of EA with the number of C_{60} can be realized by these equations. Recently density function calculations predict the EAs for the multiply

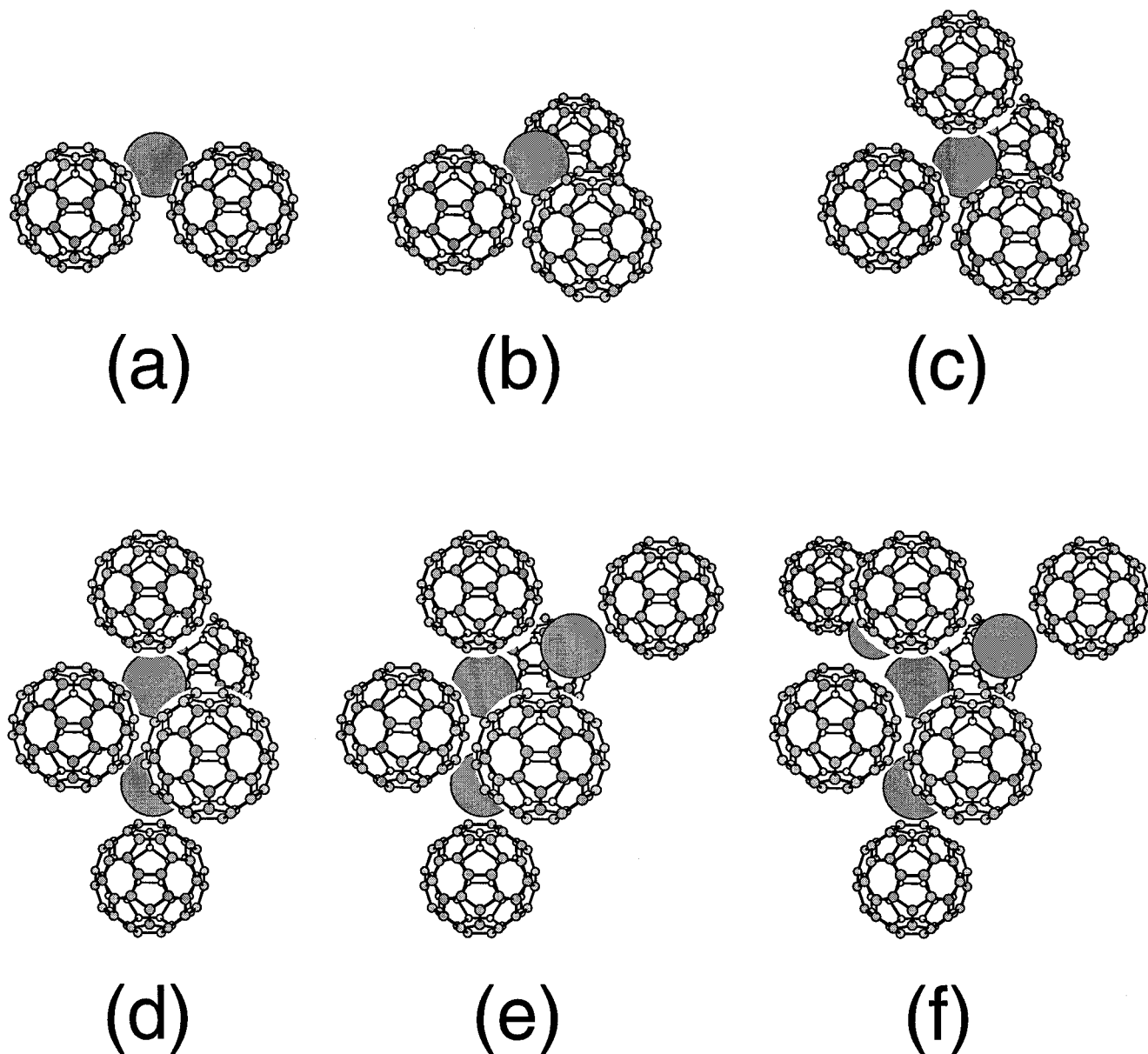


Figure 3. Proposed geometric structures; (a) $\text{Ln}_1(\text{C}_{60})_2$, (b) $\text{Ln}_1(\text{C}_{60})_3$, (c) $\text{Ln}_1(\text{C}_{60})_4$, (d) $\text{Ln}_2(\text{C}_{60})_5$, (e) $\text{Ln}_3(\text{C}_{60})_6$, and (f) $\text{Ln}_4(\text{C}_{60})_7$ ($\text{Ln} = \text{Eu}$ and Ho).

charged C_{60} , C_{60}^{x-} ($x = 1-5$).²⁸ The experimental EA difference between (1, 1) and (1, 2) for $\text{Ho}-\text{C}_{60}$ was obtained to be 0.68 eV, and the estimated value is 0.35 eV based on the predicted values. In this scheme, the EA of the (1, 4) is predicted to be more than 8 eV, which gives a reasonable explanation for there being no effective photodetachment from (1, 4)⁻ with a photon energy of 4.66 eV. In (1, 4)⁻, each C_{60}^- accepts one electron from the Ho atom and the excess charge, satisfying the charge distributions of Ho^{3+} and 4C_{60}^- . In conclusion the $\text{Ln}-\text{C}_{60}$ clusters are formed through ionic bonding, distributing the valence electrons into the ligand molecules of C_{60} .

For $\text{Eu}-\text{C}_{60}$ (Figure 5a), on the other hand, the monotonic increase in EA can similarly be rationalized by the charge distribution with Eu^{2+} , because the detached electron is released from different charged C_{60} ; C_{60}^{3-} for (1, 1)⁻, C_{60}^{2-} for (1, 2)⁻, and C_{60}^- for (1, 3)⁻. This explanation successfully leads us to the conclusion that Eu and Ho atoms in $\text{Ln}_1(\text{C}_{60})_m$ clusters take +2 and +3 oxidation states, respectively. This conclusion on the net charges of $\text{Ln}_1(\text{C}_{60})_m$ is also consistent with the following results for the formation of $\text{Ln}_n(\text{C}_{60})_m(\text{Cl})_k^+$.

For ionic clusters, it is anticipated that a chemical probe, such as the attachment of a halogen atom, can lead to insight into the charge distribution. Although the chemical method involves some ambiguity as to whether the charge distribution might result from the addition of the probing atom, the number of attached halogen atoms (k) should reflect the probable charge distribution, because a halogen atom acts as an acceptor of one electron. The maximum numbers of k (k_{max}) obtained under saturated chloridization conditions were investigated, and they are summarized in Table 2 for $\text{Ln}_n(\text{C}_{60})_m(\text{Cl})_k^+$.

For both $m = 1$ and 2, k_{max} is 1 for $\text{Eu}_1(\text{C}_{60})_m\text{Cl}_k^+$, while k_{max} is 2 for $\text{Ho}_1(\text{C}_{60})_m\text{Cl}_k^+$. The results of the k_{max} for $\text{Ln}_1(\text{C}_{60})_m\text{Cl}_k^+$ evidently indicate that Eu atoms take the oxidation state of +2, and Ho atom does that of +3, because their charge distribution can successfully be described as $\text{Eu}^{2+}_1(\text{C}_{60}^0)_m(\text{Cl}^-)_1$ and $\text{Ho}^{3+}_1(\text{C}_{60}^0)_m(\text{Cl}^-)_2$, having a neutral C_{60} . It suggests that a strong charge-charge-induced dipole interaction occurs between $\text{Eu}^{2+}/\text{Ho}^{3+}$ ion and C_{60} molecule in $\text{Ln}_1(\text{C}_{60})_m\text{Cl}_k^+$. In fact, the reported polarizability of C_{60} is very large ($\sim 80 \times 10^{-24} \text{ cm}^3$).^{29,30} For $\text{Ln}_1(\text{C}_{60})_3\text{Cl}_k^+$ ($m = 3$), however, k_{max} is 1

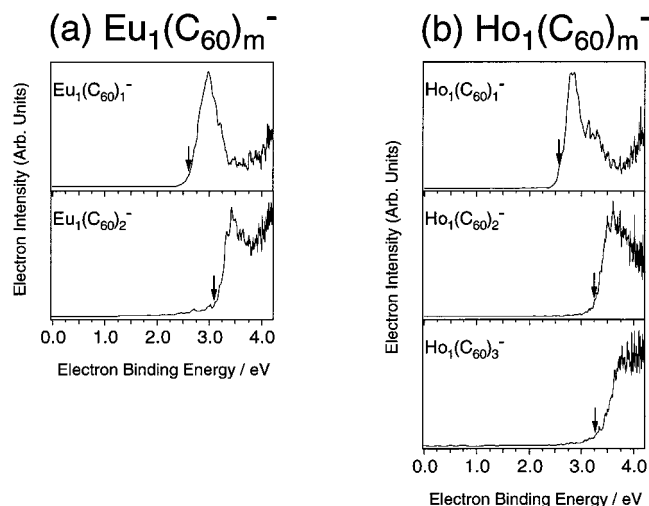
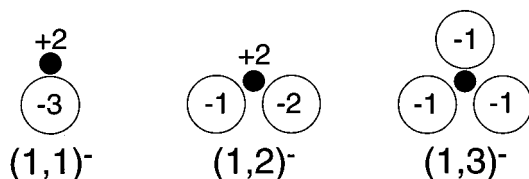


Figure 4. Photoelectron spectra of (a) $\text{Eu}_1(\text{C}_{60})_m^-$ ($m = 1$ and 2) and (b) $\text{Ho}_1(\text{C}_{60})_m^-$ ($m = 1-3$) measured at a photon energy of 4.66 eV (266 nm). The downward arrows indicate threshold energies, corresponding to adiabatic electron affinities (AEAs).

(a) Ln = Eu



(b) Ln = Ho

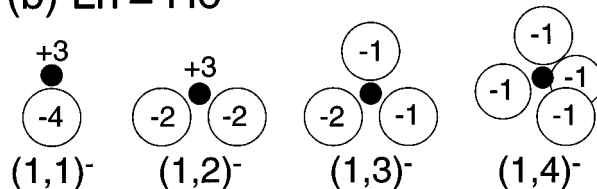


Figure 5. Allotment of valence electrons of $\text{Ln}_1(\text{C}_{60})_m^-$ are also shown schematically. These are based on the assumptions that the extra electron in $\text{Ln}_1(\text{C}_{60})_m^-$ anions is localized on C_{60} . The successful explanation for the size dependence of EAs and Cl-atom adducts indicates that Eu and Ho atoms take the oxidation states of $+2$ and $+3$, respectively.

TABLE 1: Adiabatic Electron Affinities of $\text{Ln}_1(\text{C}_{60})_m^-$ Clusters (Ln = Eu and Ho) in eV

cluster	Ln=Eu	Ln=Ho
$\text{Ln}_1(\text{C}_{60})_1$	2.61(12) ^a	2.56(12)
$\text{Ln}_1(\text{C}_{60})_2$	3.10(25)	3.24(19)
$\text{Ln}_1(\text{C}_{60})_3$	>4.0	3.25(21)
$\text{Ln}_1(\text{C}_{60})_4$	—	> 4.0

^a 2.61(12) represents 2.61 ± 0.12 .

for both Ln = Eu and Ho. According to the charge distribution with Eu^{2+} and Ho^{3+} , $\text{Ho}_1(\text{C}_{60})_3$ should attract two Cl atoms, forming $\text{Ho}^{3+}_1(\text{C}_{60})_3(\text{Cl}^-)_2$. This discrepancy is expected to be attributable to steric hindrance of $\text{Ln}_1(\text{C}_{60})_3$: the electronic repulsion Cl^- could prevent attaching the second Cl atom to $\text{Ln}_1(\text{C}_{60})_3\text{Cl}_1^+$.

For $\text{Ln}_n(\text{C}_{60})_4(\text{Cl})_k^+$ and $\text{Ln}_n(\text{C}_{60})_5(\text{Cl})_k^+$, moreover, a Cl atom can similarly be attached to them. $\text{Ln}_{n+1}(\text{C}_{60})_{n+3}^+$ and $\text{Ln}_{n+2}(\text{C}_{60})_{n+3}^+$ can attract one and two Cl atom(s) because they have one and two exterior Ln atom(s), respectively. The exterior Ln

TABLE 2: The Maximum Number of k_{max} for $\text{Ln}_n(\text{C}_{60})_m(\text{Cl})_k^+$

species		k_{max}	
n	m	Ln=Eu	Ln=Ho
1	1	1	2
1	2	1	2
1	3	1	1
1	4	0	0
2	4	1	1
3	4	2	2
2	5	0	0
3	5	1	1
4	5	2	2

atom can act as a site for the Cl-atom addition and they satisfy the charge distribution of $\text{Ln}^{2+}/\text{Ln}^{3+}$ with Cl^- ion(s).

In summary, we have reported a new class of fullerene chemistry between C_{60} and rare-earth metal atoms of Eu and Ho. This experiment reveals a new form of exohedral metallofullerenes, and photoelectron spectroscopy of the mass-selected metallofullerenes provides the information on the charge distribution; Eu and Ho atoms in the $\text{Ln}-\text{C}_{60}$ clusters take the oxidation states of $+2$ and $+3$, respectively. This gas-phase preparation of metallofullerenes has the advantage that selected precursor components can lead to novel structures of deposited materials in a controlled fashion. Since the $\text{Ln}_n(\text{C}_{60})_{n+3}$ clusters are stable toward O_2 , deposited $\text{Ln}-\text{C}_{60}$ materials might be promising to be developed even under exposure to air.

Acknowledgment. This work is supported by a program entitled “Research for the Future (RFTF)” of the Japan Society for the Promotion of Science (98P01203) and by a Grant-in-Aid for Scientific Research on Priority Areas from the Ministry of Education, Science, Sports, and Culture. Y.N. expresses his gratitude to research fellowships of the Japan Society for the Promotion of Science for Young Scientists.

References and Notes

- (1) Kroto, H. W.; Heath, J. R.; O'Brien, S. C.; Curl, R. F.; Smalley, R. E. *Nature* **1985**, *318*, 162.
- (2) Hebard, A. F.; Rosseinsky, M. J.; Haddon, R. C.; Murphy, D. W.; Glarum, S. H.; Palstra, T. T. M.; Ramirez, A. P.; Kortan, A. R. *Nature* **1991**, *350*, 600.
- (3) Tanigaki, K.; Ebbesen, T. W.; Saito, S.; Mizuki, J.; Tsai, J. S.; Kubo, Y.; Kuroshima, S. *Nature* **1991**, *352*, 222.
- (4) Heath, J. R.; O'Brien, S. C.; Zhang, Q.; Liu, Y.; Curl, R. F.; Kroto, H. W.; Tittel, F. K.; Smalley, R. E. *J. Am. Chem. Soc.* **1985**, *107*, 7779.
- (5) Chai, Y.; Cuo, T.; Jin, C.; Haufler, R. E.; Chibante, L. P. F.; Fure, J.; Wang, L.; Alford, J. M.; Smalley, R. E. *J. Phys. Chem.* **1991**, *95*, 7564.
- (6) Johnson, R. D.; De Vries, M. S.; Salem, J.; Bethune, D. S.; Yannoni, C. S. *Nature* **1992**, *355*, 239.
- (7) Shinohara, H.; Sato, H.; Ohkohchi, M.; Ando, Y.; Kodama, T.; Shida, T.; Kato, T.; Saito, Y. *Nature* **1992**, *357*, 52.
- (8) Poirier, D. M.; Knupfer, M.; Weaver, J. H.; Andreoni, W.; Laasonen, K.; Parrinello, M.; Bethune, D. S.; Kikuchi, K.; Achiba, Y. *Phys. Rev. B* **1994**, *49*, 17403.
- (9) Takahashi, T.; Ito, A.; Inakuma, M.; Shinohara, H. *Phys. Rev. B* **1995**, *52*, 13812.
- (10) Hino, S.; Takahashi, H.; Iwasaki, K.; Matsumoto, K.; Miyazaki, T.; Hasegawa, S.; Kikuchi, K.; Achiba, Y. *Phys. Rev. Lett.* **1993**, *71*, 4261.
- (11) Sakurai, T.; Wang, X. D.; Xue, Q. K.; Hasegawa, Y.; Hashizume, T.; Shinohara, H. *Prog. Surf. Sci.* **1996**, *51*, 263.
- (12) Lin, N.; Huang, H.; Yang, S.; Cue, N. *J. Phys. Chem. A* **1998**, *102*, 4411.
- (13) (a) Nagase, S.; Kobayashi, K. *Chem. Phys. Lett.* **1994**, *228*, 106. (b) Nagase, S.; Kobayashi, K.; Akasaka, T. *Bull. Chem. Soc. Jpn.* **1996**, *69*, 2131, and references therein.
- (14) Broclawik, E.; Eilmes, A. *J. Chem. Phys.* **1998**, *108*, 3498.
- (15) Bethune, D. S.; Johnson, R. D.; Salem, J. R.; De Vries, M. S.; Yannoni, C. S. *Nature* **1993**, *366*, 123.
- (16) Moro, L.; Ruoff, R. S.; Becker, C. H.; Lorents, D. C.; Malhotra, R. *J. Phys. Chem.* **1993**, *97*, 6801.
- (17) Huang, R.; Lu, W.; Yang, S. *J. Chem. Phys.* **1995**, *102*, 189.

- (18) Odas, E.; Kortan, A. R.; Kopylov, N.; Ramirez, A. P.; Siegrist, T.; Rabe, K. M.; Bair, H. E.; Schuppler, S.; Citrin, P. H. *Nature* **1995**, 375, 126.
- (19) Nonose, S.; Sone, Y.; Onodera, K.; Sudo, S.; Kaya, K. *J. Phys. Chem.* **1990**, 94, 2744.
- (20) (a) Nakajima, A.; Nagao, S.; Takeda, H.; Kurikawa, T.; Kaya, K. *J. Chem. Phys.* **1997**, 107, 6491. (b) Kurikawa, T.; Nagao, S.; Miyajima, K.; Nakajima, A.; Kaya, K. *J. Phys. Chem. A* **1998**, 102, 1743. (c) Nagao, S.; Kurikawa, T.; Miyajima, K.; Nakajima, A.; Kaya, K. *J. Phys. Chem. A* **1998**, 102, 4495.
- (21) Harberland, H. *Clusters of Atoms and Molecules*; Springer-Verlag: Berlin, 1994; p 230.
- (22) Geusic, M. E.; Morse, M. D.; O'Brien, S. C.; Smalley, R. E. *Rev. Sci. Instrum.* **1985**, 56, 2123.
- (23) Nakajima, A.; Taguwa, T.; Hoshino, K.; Sugioka, T.; Naganuma, T.; Ono, F.; Watanabe, K.; Nakao, K.; Konishi, Y.; Kishi, R.; Kaya, K. *Chem. Phys. Lett.* **1993**, 214, 22.
- (24) Hotop, H.; Lineberger, W. C. *J. Phys. Chem. Ref. Data* **1975**, 4, 539.
- (25) Esaulov, V. A. *Ann. Phys. Fr.* **1986**, 11, 493.
- (26) (a) Hoshino, K.; Kurikawa, T.; Takeda, H.; Nakajima, A.; Kaya, K. *J. Phys. Chem.* **1995**, 99, 3053. (b) Kurikawa, T.; Hirano, M.; Takeda, H.; Yagi, K.; Hoshino, K.; Nakajima, A.; Kaya, K. *J. Phys. Chem.* **1995**, 99, 16248. (c) Kurikawa, T.; Takeda, H.; Nakajima, A.; Kaya, K. *Z. Phys. D* **1997**, 40, 65. (d) Weis, P.; Kemper, P. R.; Bowers, M. T. *J. Phys. Chem. A* **1997**, 101, 8207. (e) Kurikawa, T.; Takeda, H.; Hirano, M.; Judai, K.; Arita, T.; Nagao, S.; Nakajima, A.; Kaya, K. *Organometallics* **1999**, 18, 1430.
- (27) (a) Kurikawa, T.; Negishi, Y.; Hayakawa, F.; Nagao, S.; Miyajima, K.; Nakajima, A.; Kaya, K. *J. Am. Chem. Soc.* **1998**, 120, 11766. (b) Miyajima, K.; Kurikawa, T.; Hashimoto, M.; Nakajima, A.; Kaya, K. *Chem. Phys. Lett.* **1999**, 306, 256.
- (28) Green, W. H., Jr; Gorun, S. M.; Fitzgerald, G.; Fowler, P. W.; Ceulemans, A.; Titeca, B. C. *J. Phys. Chem.* **1996**, 100, 14892.
- (29) Bonin, K. D.; Kadar-Kallen, M. A. *Int. J. Mod. Phys.* **1994**, 8, 3313.
- (30) Antoine, R.; Dugourd, Ph.; Rayane, D.; Benichou, E.; Broyer, M.; Chandezon, F.; Guet, C. *J. Chem. Phys.* **1999**, 110, 9771.